Research Article

Journal of PeptideScience

Received: 18 July 2008 Revised: 17 October 2008 Accepted: 20 October 2008 Published online in Wiley Interscience: 8 December 2008

(www.interscience.com) DOI 10.1002/psc.1097

Regulatory elements and functional implication for the formation of dimeric visinin-like protein-1

Ku-Chung Chen, Li-Kuan Wang and Long-Sen Chang*

Size exclusion chromatographic analyses showed that Ca^{2+}-free VILIP-1 contained both monomeric and dimeric forms, while no appreciable dimerization was noted with Ca^{2+}-free VILIP-3. Swapping of EF-hands 3 and 4 of VILIP-1 with those of VILIP-3 caused the inability of the resulting chimeric protein to form dimeric protein. Nonreducing SDS-PAGE analyses revealed that most of the dimeric VILIP-1 was noncovalently bound together. Reduced glutathione (GSH)/oxidized glutathione (GSSG) treatment notably enhanced the formation of disulfide-linked VILIP-1 dimer, while Ca^{2+} and Mg^{2+} enhanced disulfide dimerization of VILIP-1 marginally in the presence of thiol compounds. Cys-187 at the C-terminus of VILIP-1 contributed greatly to form S-S-crosslinked dimer as revealed by mutagenesis studies. The ability of GSH/GSSG-treated VILIP-1 to activate guanylyl cyclase B was reduced by substituting Cys-187 with Ala. Together with disulfide dimer of VILIP-1 detected in rat brain extracts, our data may imply the functional contribution of disulfide dimer to the interaction of VILIP-1 with its physiological target(s).

Keywords: VILIP-1; mutagenesis; dimerization; disulfide bond

Introduction

Neuronal calcium sensor (NCS) proteins can be divided into five groups according to their sequence similarity. They are guanylyl cyclase-activating proteins (GCAPs), recoverins, NCS-1 (also known as frequenin), visinin-like proteins (VILIPs) and K^+ channel-interacting proteins (KChIPs) [1,2]. All the NCS proteins share fourconserved EF-hand motifs, but only two or three can bind Ca^{2+}. Most of them possess a consensus myristoylation sequence at the N-terminus.

The VILIP family is composed of VILIP-1, VILIP-2, VILIP-3, hippocalcin and neurocalcin δ, which share a high degree of amino acid similarity. VILIP-1 is expressed primarily in the brain, while lower expression in some peripheral organs including heart, testis, ovary and colon is reported [3]. VILIP-1 is found to increase cell-surface expression of α4- and β2-subunits of the neuronal nicotinic acetylcholine receptor in tsA201 cell [4]. In addition, VILIP-1 has been shown to increase cGMP levels by acting directly on guanylyl cyclase B [5,6]. Moreover, overexpression of VILIP-1 results in a cAMP-mediated decrease in invasiveness of squamous carcinoma cells [7,8]. Recent studies indicate that VILIP-1 modulates the activity of guanylyl cyclase B through clathrin-dependent cycling and enhances insulin secretion in pancreatic β-cells [6,9]. Nevertheless, the underlying mechanism associated with how the molecular structure regulates multiple functions of VILIP-1 remains unclear.

Previous research shows that GCAP-1 and GCAP-2 undergo reversible dimerization upon dissociation of Ca^{2+}, and the ability of GCAP-2 to activate photoreceptor membrane guanylyl cyclase correlates with the formation of dimeric forms [10]. Alternatively, dimerization affects the binding of KChIP3 with targeted DNA and the resultant gene expression [11,12]. These findings suggest that the biological activities of NCS proteins could be functionally altered by changes in their molecular structure. The present study is carried out in order to elucidate whether VILIPs form oligomeric structures.

Materials and Methods

Construction of Chimeric and Mutated VILIPs

pET22b(+) plasmids containing cDNAs of human VILIP1 (NM_003385) and VILIP3 (NM_002149) were prepared in our laboratory as previously described [13]. Figure 1 shows PCR primers used in the present study and preparation of chimeric and mutated VILIPs by overlapping PCR reaction. To subclone VILIP-1 and VILIP-3 into pET22b(+), sense (VILIP-1 up primer, 5′-CATATGGGGAAGCAGAATAGCAAACTGGC-3′; VILIP-3 up primer, 5′-CATATGGGCAAACAGAACAGCAAGCTG-3′; the underlines indicate *Nde*I site) and antisense primers (VILIP-1 down primer, 5′-GTCGACTCATTTCTGGATCTCGCACTGCAG-3′; VILIP-3 down primer, 5′-GTCGACTCAGAACTGACTGGCAC TGCTGGG-3′; the underlines indicate *Sal*I site) were synthesized. To prepare truncated and mutated VILIPs, the primers (V-13 up primer, 5′-CTTTGAGCAGAAACTTAATTGGGCCTTCAGC-3′; V-13 down primer, 5′-GCTGAAGGCCCAATTAAGTTTCTGCTCAAAG-3′; V-31 up primer, 5′-GCTGGAGCAGAAACTTAACTGGGC-3′; V-31 down primer, 5′-ATTGAAGGCCCAGTTAAGTTTCTGCTCCAGCT-3′; V1-C187A, 5′-GTCGACTCATTTCTGGATGTCTGCCTGCAGAAGTAA-3′) were used. PCR-amplified fragments of V-13 (EF-hands 1–2

* *Correspondence to: Long-Sen Chang, Institute of Biomedical Sciences, National Sun Yat-Sen University, Kaohsiung 804, Taiwan.*
E-mail: lschang@mail.nsysu.edu.tw

Institute of Biomedical Sciences, National Sun Yat-Sen University-Kaohsiung Medical University Joint Research Center, National Sun Yat-Sen University, Kaohsiung 804, Taiwan

A

Primer	Sequence
VILIP-1 up primer	5' cat atg ggg aag cag aat agc aaa ctg gc 3'
VILIP-1 down primer	5' gtc gac tca ttt ctg gat ctc gca ctg cag 3'
VILIP-3 up primer	5' cat atg ggc aaa cag aac agc aag ctg 3'
VILIP-3 down primer	5' gtc gac tca gaa ctg act ggc act gct ggg 3'
V-13 up primer	5' ctt tga gca gaa act taa ttg ggc ctt cag c 3'
V-13 down primer	5' gct gaa ggc cca att aag ttt ctg ctc aaa g 3'
V-31 up primer	5' gct gga gca gaa act taa ctg ggc 3'
V-31 down primer	5' att gaa ggc cca gtt aag ttt ctg ctc cag ct 3'
V1-C187A	5' gtc gac tca ttt ctg gat gtc tgc ctg cag aag taa 3'

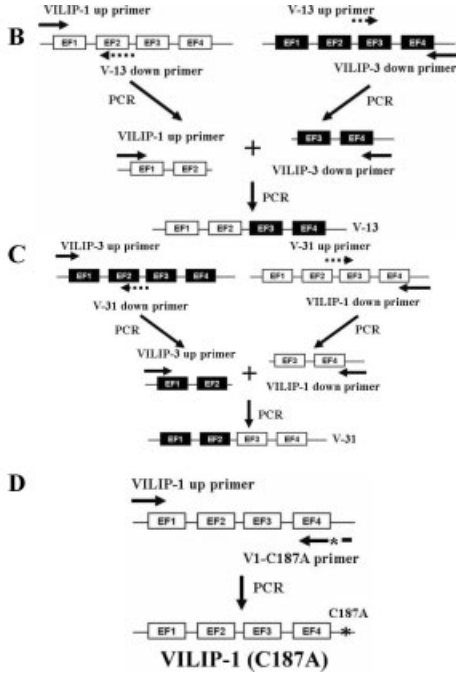

Figure 1. Schematic drawings showing preparation of chimeric and mutated VILIPs. (A) The primers used for preparing the cDNAs of chimeric and mutated VILIPs. V-13 (B), V-31 (C) and VILIP-1(C187A) (D) were prepared using overlapping PCR reaction.

of VILIP-1 and EF-hands 3–4 of VILIP-3), V-31 (EF-hands 1–2 of VILIP-3 and EF-hands 3–4 of VILIP-1) and VILIP-1(C187A) were cloned into pGEM-T easy vector using TA-cloning kit (Promega). The cDNAs encoding chimeric and mutated VILIPs were confirmed by DNA sequencing. The fragments were subcloned into *Nde*I/*Sal*I-digested pET22b(+) plasmids.

Preparation of Recombinant VILIPs

To prepare myristoylated VILIPs, cDNA of VILIPs was subcloned into pET22b(+) and either transformed alone or cotransformed with pBB131 encoding N-myristoyltransferase (kindly provided by Dr. Jeffery Gordon, Washington University, St. Louis, MO) into competent *E. coli* BL21(DE3) cells. Induction of gene expression was performed essentially according to the procedure described in [14]. For preparation of myristoylated VILIPs, 5 mg/l myristic acid was added until OD_{550} reached 0.5.

Bacterial extracts were loaded onto a DEAE-Sephacel column (3 × 10 cm) equilibrated with 50 mM Tris-HCl (pH 7.5) containing 1 mM EDTA and 1 mM DTT, and eluted with a linear gradient of 600 ml from 0 to 0.1 M NaCl in the same buffer. The flow rate was 2 ml/min, and the eluent was monitored at 280 nm. The products were analyzed by SDS-PAGE, and protein concentration was determined by Bradford assay.

Analysis of Oligomeric VILIPs Using Size Exclusion Chromatography

The formation of oligomer was analyzed using a Hiprep™ 16/60 Sephacryl™ S-200 column (1.6 × 60 cm) equilibrated with 20 mM Tris-HCl (pH 7.5) containing 1 mM DTT, 50 mM KCl and 100 mM NaCl with the addition of 1 mM EDTA, 0.5 mM $MgCl_2$ or 0.1 mM $CaCl_2$, respectively. Proteins were eluted with the same buffer at a flow rate of 0.25 ml/min. Molecular mass standards comprising albumin (67 kDa), ovalbumin (43 kDa), chymotrypsinogen A (25 kDa), and RNase A (13.7 kDa) were used for calibration.

GSH/GSSG-Induced Disulfide Dimerization of VILIPs

VILIP-1, or mutants (10 µg), were dissolved in 20 µl of 50 mM Tris-HCl (pH 8.0) containing 5 mM GSH and 0.05 mM GSSG in the presence of 1 mM EDTA, 0.5 mM $MgCl_2$ or 0.1 mM $CaCl_2$, respectively. The used concentration of GSH, GSSG, Mg^{2+} and Ca^{2+} was within the range of their physiological concentration. The reaction was allowed to proceed for 24 h, and the samples were withdrawn for nonreducing SDS-PAGE and Western blotting analyses. Anti-VILIP-1 antibodies were prepared by immunizing rabbits with myristoylated VILIP-1, and the antisera were further purified by VILIP-1-Sepharose column. Coupling of myristoylated VILIP-1 to CNBr-activated Sepharose 4B (GE Healthcare) was carried out according to manufacturer's protocol. Western blotting analyses revealed that the purified anti-VILIP-1 antibodies did not show cross-reactivity toward myristoylated VILIP-3 (data not shown).

Identification of S-S-crosslinked VILIP-1 Dimer in Rat Brain Extracts

Rat brain tissues including cerebrum, cerebellum, brain stem and hippocampus were homogenized in 50 mM Tris-HCl (pH 7.5) containing 100 mM NaCl, 50 mM KCl and 0.1 mM PMSF. After removal of nuclei and cellular debris by centrifugation at 1000 × g for 5 min, the supernatants were further centrifuged at 20 000 × g for 20 min at 4 °C. The supernatant (cytosolic fraction) and the pellet (membrane fraction) were subjected to SDS-PAGE and Western blotting analyses.

In Vitro Guanylyl Cyclase Activity Assay

Rat C6 glioma cells were maintained in DMEM containing 10% fetal calf serum, penicillin/streptomycin (100 µg/ml) and 1% glutamine in a humidified atmosphere of 5% CO_2 at 37 °C. Cells were harvested by centrifugation at 1000 × g for 15 min at 4 °C, and

Journal of PeptideScience

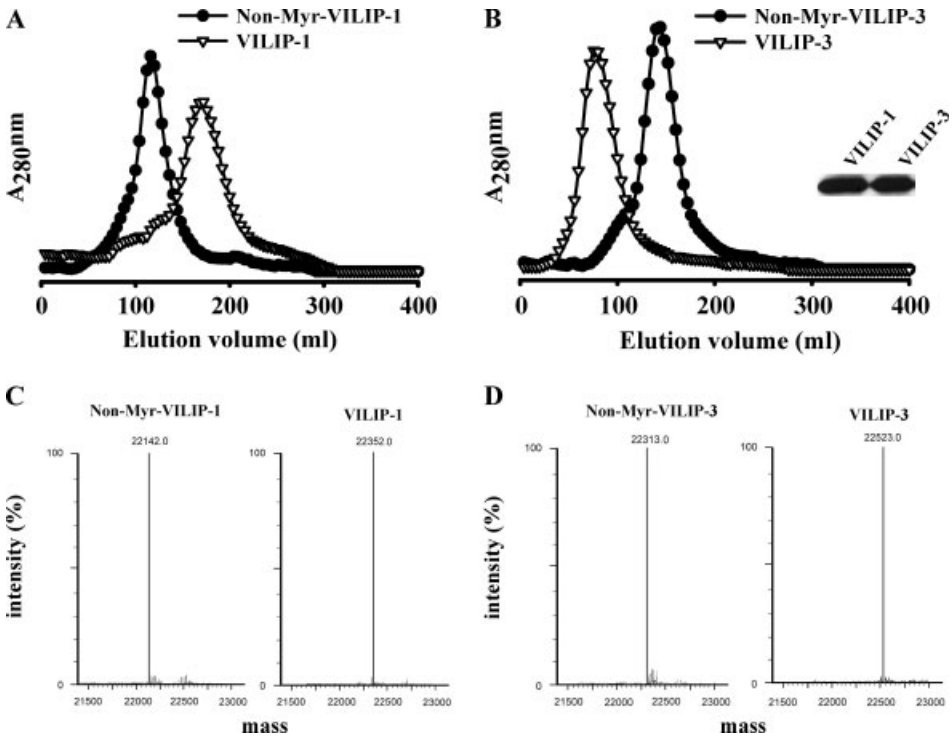

Figure 2. Purification of VILIP-1 and VILIP-3 on DEAE-Sephacel columns. Nonmyristoylated and myristoylated VILIPs (A, VILIP-1; B, VILIP-3) were applied on DEAE-Sephacel columns equilibrated with 50 mM Tris-HCl (pH 7.5) containing 1 mM EDTA and 1 mM DTT, and eluted with a linear gradient of 600 ml from 0 to 0.1 M NaCl in the same buffer at a flow rate of 2 ml/min. Inset: SDS-PAGE analyses showing homogeneity of purified myristoylated VILIP-1 and VILIP-3. VILIP is the abbreviation of myristoylated VILIP, while Non-Myr-VILIP represents nonmyristoylated VILIP. (C) Mass analyses of Non-Myr-VILIP-1 and VILIP-1. (D) Mass analyses of Non-Myr-VILIP-3 and VILIP-3.

resuspended in the buffer constituted with 20 mM HEPES, pH 7.5, 10 mM NaCl, 50 mM KCl, 0.1 mM PMSF, 1 mM benzamidine hydrochloride, 1 mM 3-isobutyl-1-methylxanthine, 0.1 mM $CaCl_2$ and 0.5 mM $MgCl_2$. VILIPs were incubated with 50 mM Tris-HCl (pH 8.0) containing 5 mM GSH/0.05 mM GSSG in the presence of 0.5 mM Mg^{2+} and 0.1 mM Ca^{2+} for 24 h. Cell membrane fraction extracted from 4×10^6 cells was incubated with 20 μM GSH/GSSG-treated VILIPs for 30 min at 37 °C. After the addition of 0.2 μM CNP and 1 mM GTP, the reaction was allowed to proceed for 5 min at 37 °C. Generated cGMP was extracted with 65% ethanol and detected using ELISA assay kit (GE Healthcare).

Statistical Analysis

All data are presented as mean ± SD. Significant differences among the groups were determined using the unpaired Student's *t*-test. A value of $P < 0.05$ was taken as an indication of statistical significance. All the figures shown in this article were obtained from at least three independent experiments with similar results.

Other Tests

SDS-PAGE analyses and Western blotting analyses were carried out essentially according to the methods previously described [14].

Results and Discussion

Figure 2 shows that nonmyristoylated VILIPs (Non-Myr-VILIPs) and myristoylated VILIPs were purified on DEAE-Sephacel columns, and eluted out from DEAE-Sephacel column at different times. For

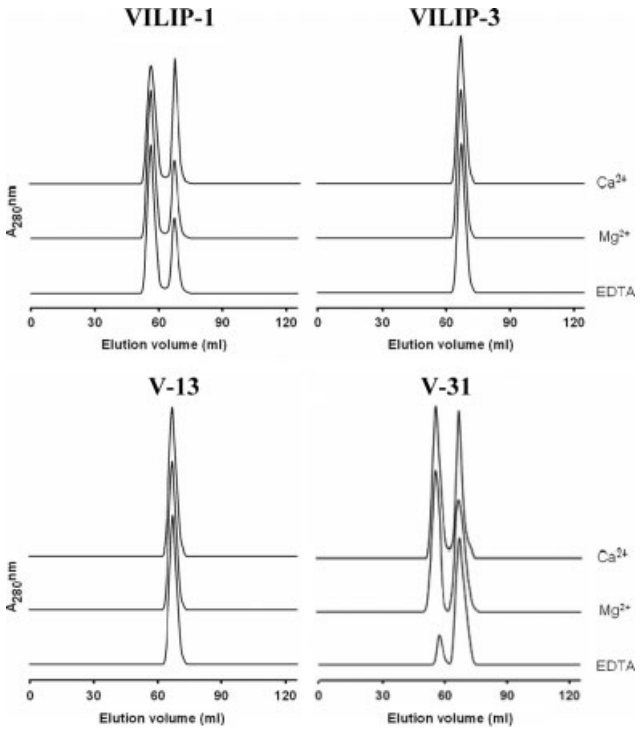

Figure 3. Size exclusion chromatography showing dimerization of VILIP-1 and V-31. Myristoylated VILIPs were applied on a Hiprep 16/60 Sephacryl S-200 column (1.6 × 60 cm) equilibrated with 20 mM Tris-HCl (pH 7.5) containing 1 mM DTT, 50 mM KCl, 100 mM NaCl with the addition of 1 mM EDTA, 0.5 mM Mg^{2+}, or 0.1 mM Ca^{2+}, respectively. The flow rate was 0.25 ml/min.

simplicity, VILIP represents myristoylated protein in this paper. It was worth noting that Non-Myr-VILIP-1 eluted by lower NaCl concentration than VILIP-1, whereas Non-Myr-VILIP-3 eluted by higher NaCl concentration than VILIP-3. This likely reflected that myristoylation differently altered the conformation of VILIP-1 and VILIP-3, and thus, the binding of VILIP-1 and VILIP-3 with DEAE-Sephacel column. The homogeneity of purified VILIP-1 and VILIP-3 were verified by SDS-PAGE, and a 210 Dalton-raised increase in molecular weight due to incorporation of myristoyl group at the N-terminus was proved using mass spectrometry (Figure 2(C) and (D)).

Size exclusion chromatography showed that VILIP-1 formed a dimeric structure regardless of whether Ca^{2+} was present or not (Figure 3). Dimerization of VILIP-1 was enhanced by both Ca^{2+} and Mg^{2+}. Alternatively, dimerization of VILIP-3 was not observed. In order to verify the region within VILIP-1 responsible for stabilizing dimeric form, chimeric V-13 and V-31 were prepared. In contrast to V-13, V-31 was found to form dimeric structure, suggesting that the intact EF-hands 3 and 4 were related to the formation of dimeric VILIP-1. Moreover, dimerization of V-31 was notably enhanced by Mg^{2+} and Ca^{2+}.

Previous studies showed that Ca^{2+} modulated the formation of dimeric recoverin, and the dimer was linked with an intermolecular disulfide bond [15]. In order to assess whether dimeric VILIP-1 was linked by the disulfide bond, VILIP-1 was subjected to SDS-PAGE analysis under reducing and nonreducing conditions. Figure 4(A) shows that only a little amount of VILIP-1 was disulfide-linked VILIP-1 dimer. Incubation with GSH/GSSG can further increase the production of disulfide dimer. Maximal conversion from monomer to disulfide dimer was achieved after incubation with GSH/GSSH for 24 h (Inset of Figure 4(A)). Regardless of the absence or presence of thiol compounds, the production of disulfide dimer was further increased when Ca^{2+} and Mg^{2+} were added (Figure 4(B)). Compared with Mg^{2+} and Ca^{2+}, GSH/GSSG greatly induced the formation of dimeric VILIP-1.

In contrast to that by VILIP-1, the formation of disulfide dimer by VILIP-3 in the presence of GSH/GSSG was insignificant (Figure 4(C)). After treatment with GSH/GSSG, the amount of S-S-linked V-31 dimer was notably higher than that of V-13, reflecting that the Cys residue(s) located at C-terminal half of VILIP-1 should greatly contribute to the formation of disulfide dimer (Figure 4(C)). Given that V-31 contains Cys-187 of VILIP-1, and V-13 contains Cys-38 and Cys-87 of VILIP-1, it is likely to suggest that Cys-187 is heavily involved in forming the intermolecular disulfide bond. This suggestion was proved by the finding that substitution of Cys-187 with Ala by mutagenesis drastically reduced the production of disulfide dimer from 45 to 12%. Nevertheless, the appearance

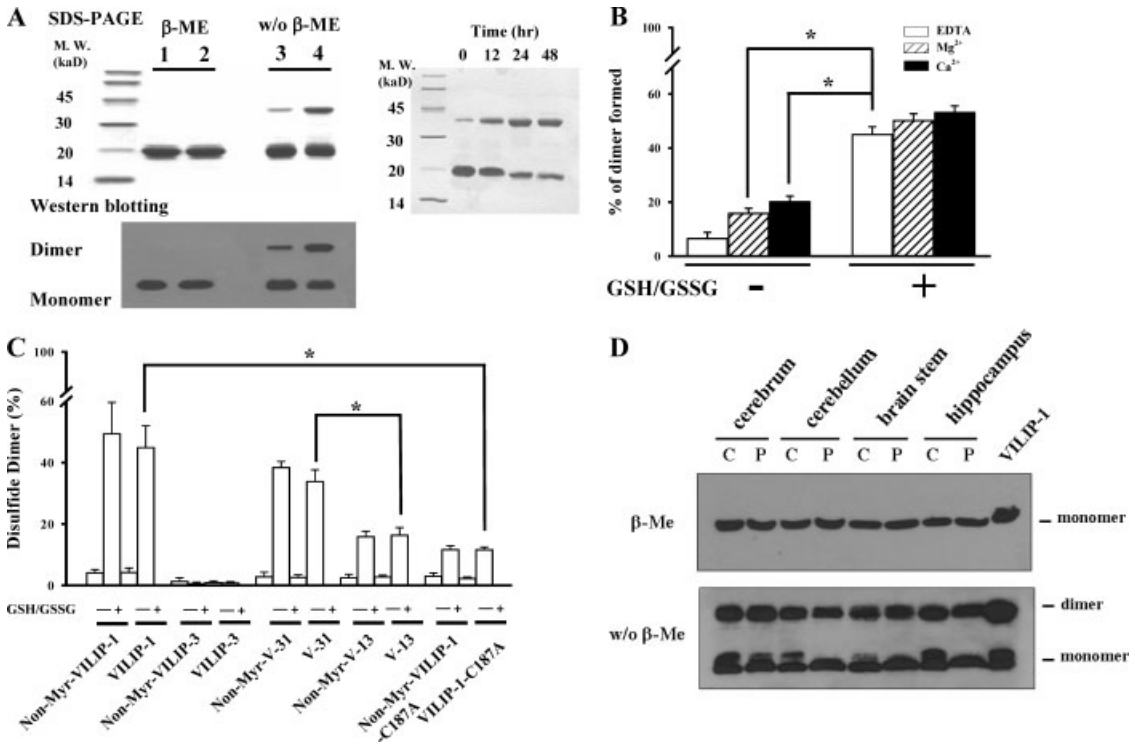

Figure 4. GSH/GSSG treatment enhanced the formation of disulfide-linked VILIP-1 dimer. (A) SDS-PAGE analyses of VILIP-1 and GSH/GSSG-treated VILIP-1. (Top panel) VILIP-1 (10 μg) was incubated with 50 mM Tris-HCl-1 mM EDTA (pH 8.0) in the absence (lanes 1 and 3) or presence (lanes 2 and 4) of 5 mM GSH/0.05 mM GSSG for 12 h, and the reaction mixtures were then subjected to reducing and nonreducing SDS-PAGE. (Bottom panel) Western blotting analysis showing the immunoreactivity of dimeric protein toward anti-VILIP-1 antibodies. Inset: SDS-PAGE analyses of VILIP-1 after treatment with 5 mM GSH/0.05 mM GSSG for 12, 24 and 48 h, respectively. (B) The effect of GSH/GSSG, Ca^{2+} and Mg^{2+} on the formation of S-S-crosslinked VILIP-1 dimer. VILIP-1 (10 μg) was incubated with 50 mM Tris-HCl (pH 8.0) containing 5 mM GSH/0.05 mM GSSG in the presence of 1 mM EDTA, 0.5 mM Mg^{2+} or 0.1 mM Ca^{2+}, respectively. The mixtures were allowed to stand at room temperature for 24 h. The results of nonreducing SDS-PAGE were analyzed by densitometry. Results are represented as the mean ± SD of three independent experiments. (*$P < 0.05$) (C) Disulfide dimerization of chimeric and mutated VILIPs. Chimeric and mutated VILIPs were incubated with 50 mM Tris-HCl (pH 8.0) containing 5 mM GSH/0.05 mM GSSG and 1 mM EDTA for 24 h. The results of nondenaturing SDS-PAGE were analyzed using a densitometer. Results are mean ± SD for triplicate determinations. (*$P < 0.05$) Myristoylation did not significantly affect the formation of disulfide dimer. (D) The cytosol and membrane fractions from rat cerebrum, cerebellum, brain stem and hippocampus were analyzed by Western blotting analyses after reducing (Top panel) or nonreducing (bottom panel) SDS-PAGE. C and P represent cytosolic and membrane fractions, respectively.

Journal of PeptideScience

of VILIP-1(C187A) dimer inferred that Cys-38 and/or Cys-87 also formed disulfide linkage(s) in dimeric VILIP-1. In the meantime, the ability of nonmyristoylated VILIPs to form disulfide dimer was not significantly different from that of their myristoylated cognate. It was evident that myristoylation did not affect the formation of disulfide dimer. As shown in Figure 4(D), disulfide dimer of VILIP-1 was identified in rat brain extracts, implying that the conversion between monomer and disulfide dimer may play a physiological role in governing the biological activity of VILIP-1.

Previous studies report that VILIP-1 modulates cGMP signalling pathways through guanylyl cyclase B either in transfected neural cells or in cerebellar granule neurons [5]. Given that Glioma C6 cells had been reported to possess intrinsic guanylyl cyclase B, cell membrane fractions from C6 cells were used for *in vitro* guanylyl cyclase activity assay. As shown in Figure 5(A), GSH/GSSG-treated VILIP-1 increased the production of cGMP in a dose-dependent manner. A maximal production of cGMP was observed after incubation with 10 μM GSH/GSSG-treated VILIP-1 (Figure 5(A)). As shown in Figure 5(B), GSH/GSSG-treated VILIP-1 and V-13 induced cGMP generation, while GSH/GSSG-treated VILIP-3 and V-31 were unable to activate guanylyl cyclase B. These results implied that N-terminal half of VILIP-1 may play a role in regulating guanylyl cyclase B activity. In fact, EF-hand 1 of GCAP-1 has been proved to be functionally important for activating and interacting with guanylate cyclase [16]. Compared with GSH/GSSG-treated VILIP-1, GSH/GSSG-treated VILIP-1(C187A) showed a reduction in activating guanylyl cyclase B activity. cGMP generation induced by VILIP-1 (Figure 5(A)) without pretreatment with GSH/GSSG was indistinguishable from that of GSH/GSSG-treated VILIP-1(C187A). Apparently, disulfide dimer of VILIP-1 may functionally enhance guanylyl cyclase B activity.

Previous studies suggest that the biological activities of GCAPs and KChIP3 are modulated by switch of oligomeric structure [10–12,17]. Ca^{2+}-loaded GCAP-2 is a monomeric form and forms a dimer upon dissociation of Ca^{2+} [10]. Upon binding with Ca^{2+}, tetrameric KChIP3 converts into a dimeric Ca^{2+}-bound KChIP3. Moreover, Mg^{2+} is found to regulate the activity of GCAP-1 and KChIP3 [12,17]. Although Mg^{2+} stabilizes monomeric KChIP3, it does not exert any influence on the formation of oligomeric GCAP-1. Noticeably, the binding forces for maintaining oligomeric GCAPs and KChIP3 are noncovalent ones. Alternatively, intermolecular disulfide linkage is found to stabilize Ca^{2+}-loaded recoverin dimer [15]. Nonetheless, there is no evidence supporting the appearance of oligomeric recoverin, GCAPs and KChIP3 *in vivo*. The present study is thus the first report showing that disulfide dimer of NCS protein exists physiologically. The finding that reduction in the extent of disulfide isomerization by substitution of Cys-187 with Ala causes a decrease in activating guanylyl cyclase B activity functionally implies the role of disulfide dimer *in vivo*. Sequence alignments of VILIP-3 and VILIP-1 show that VILIP-3 contains a Cys-185 located at the homologous position corresponding to Cys-187 of VILIP-1. The inability of VILIP-3 to form disulfide dimer suggests that both C-terminal half and Cys-187 of VILIP-1 are structurally essential for the formation of disulfide dimer. Since GSH and GSSG are well known for their role in facilitating disulfide formation and disulfide reshuffling [18], it is plausible that the formation of intermolecular disulfide bonds in VILIP-1 dimer is accelerated by GSH and GSSG. Given that loading with Ca^{2+} and Mg^{2+} alters the global structure of NCS proteins [10–12,15,17,19], the spatial positions of Cys residues in Ca^{2+}- or Mg^{2+}-bound VILIP-1 may approximate, which consequently increases the extent of disulfide formation. In sum, intrinsically structural factors and extrinsic

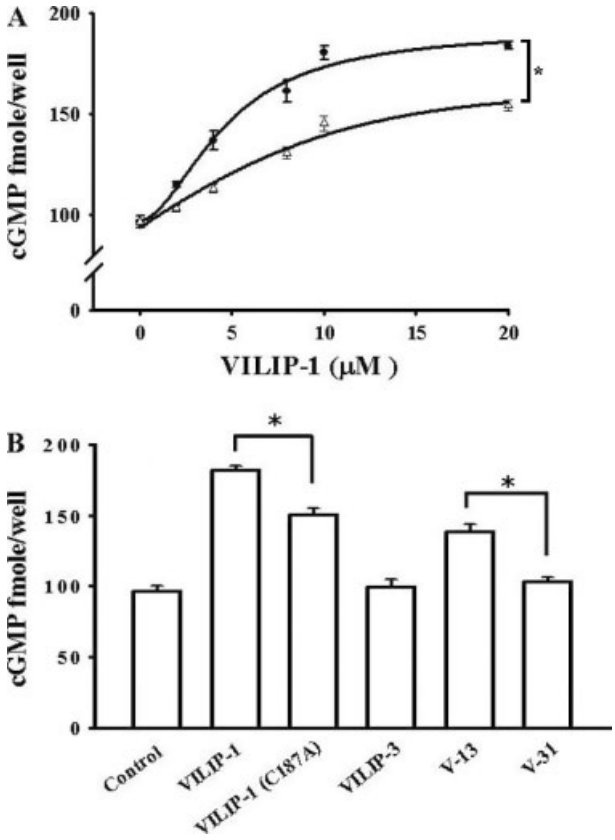

Figure 5. The ability of chimeric and mutated VILIPs to regulate guanylyl cyclase B activity. Guanylyl cyclase B activity was determined according to the procedure described in Materials and Methods Section. VILIPs were incubated with 50 mM Tris-HCl (pH 8.0) containing 5 mM GSH, 0.05 mM GSSG, 0.5 mM Mg^{2+} and 0.1 mM Ca^{2+} for 24 h. (A) Dose-dependence of VILIP-1 and GSH/GSSG-treated VILIP-1 on cGMP generation. The symbols ○ and ● represent VILIP-1 and GSH/GSSG-treated VILIP-1, respectively. (B) GSH/GSSG-treated chimeric and mutated VILIPs exhibited different ability in enhancing the activity of guanylyl cyclase B. The used concentration of VILIPs and mutated VILIPs was 20 μM. Results are mean ± SD for triplicate determinations (*$P < 0.05$).

factors including GSH/GSSG, Ca^{2+} and Mg^{2+} should coordinate with each other to complete disulfide dimerization of VILIP-1.

Acknowledgments

This work was supported by grant NSC95-2320-B110-007-MY3 from the National Science Council, ROC (to L.S. Chang), and a grant from the National Sun Yat-Sen University-Kaohsiung Medical University Joint Research Center.

References

1. Braunewell KH, Gundelfinger ED. Intracellular neuronal calcium sensor proteins: a family of EF-hand calcium-binding proteins in search of a function. *Cell Tissue Res.* 1999; **295**: 1–12.
2. Burgoyne RD, O'Callaghan DW, Hasdemir B, Haynes LP, Tepikin AV. Neuronal Ca^{2+}-sensor proteins: multitalented regulators of neuronal function. *Trends Neurosci.* 2004; **27**: 203–209.
3. Gierke P, Zhao C, Brackmann M, Linke B, Heinemann U, Braunewell KH. Expression analysis of members of the neuronal calcium sensor protein family: combining bioinformatics and Western blot analysis. *Biochem. Biophys. Res. Commun.* 2004; **323**: 38–43.

4. Lin L, Jeanclos EM, Treuil M, Braunewell KH, Gundelfinger ED, Anand R. The calcium sensor protein visinin-like protein-1 modulates the surface expression and agonist sensitivity of the $\alpha 4\beta 2$ nicotinic acetylcholine receptor. *J. Biol. Chem.* 2002; **277**: 41872–41878.
5. Braunewell KH, Brackmann M, Schaupp M, Spilker C, Anand R, Gundelfinger ED. Intracellular neuronal calcium sensor (NCS) protein VILIP-1 modulates cGMP signalling pathways in transfected neural cells and cerebellar granule neurons. *J. Neurochem.* 2001; **78**: 1277–1286.
6. Brackmann M, Schuchmann S, Anand R, Braunewell KH. Neuronal Ca^{2+} sensor protein VILIP-1 affects cGMP signalling of guanylyl cyclase B by regulating clathrin-dependent receptor recycling in hippocampal neurons. *J. Cell Sci.* 2005; **118**: 2495–2505.
7. Mahloogi H, Gonzalez-Guerrico AM, Lopez DC, Bassi DE, Goodrow T, Braunewell KH, Klein-Szanto AJ. Overexpression of the calcium sensor visinin-like protein-1 leads to a cAMP-mediated decrease of in vivo and in vitro growth and invasiveness of squamous cell carcinoma cells. *Cancer Res.* 2003; **63**: 4997–5004.
8. Gonalez-Guerrico AM, Jaffer ZM, Page RE, Braunewell KH, Chernoff J, Klein-Szanto AJ. Visinin-like protein-1 is a potent inhibitor of cell adhesion and migration in squamous carcinoma cells. *Oncogene* 2005; **24**: 2307–2316.
9. Dai FF, Zhang Y, Kang Y, Wang Q, Gaisano HY, Braunewell KH, Chan CB, Wheeler MB. The neuronal Ca^{2+} sensor protein visinin-like protein-1 is expressed in pancreatic islets and regulates insulin secretion. *J. Biol. Chem.* 2006; **281**: 21942–21953.
10. Olshevskaya EV, Ermilov AN, Dizhoor AM. Dimerization of guanylyl cyclase-activating protein and a mechanism of photoreceptor guanylyl cyclase activation. *J. Biol. Chem.* 1999; **274**: 25583–25587.
11. Osawa M, Tong KI, Lilliehook C, Wasco W, Buxbaum JD, Cheng HY, Penninger JM, Ikura M, Ames JB. Calcium-regulated DNA binding and oligomerization of the neuronal calcium-sensing protein, Calsenilin/DREAM/KChIP3. *J. Biol. Chem.* 2001; **276**: 41005–41013.
12. Osawa M, Dace A, Tong KI, Valiveti A, Ikura M, Ames JB. Mg^{2+} and Ca^{2+} differentially regulate DNA binding and dimerization of DREAM. *J. Biol. Chem.* 2005; **280**: 18008–18014.
13. Jheng FF, Wang L, Lee L, Chang LS. Functional contribution of Ca^{2+} and Mg^{2+} to the intermolecular interaction of visinin-like proteins. *Protein J.* 2006; **25**: 250–256.
14. Chang LS, Chen CY, Wu TT. Functional implication with the metal-binding properties of KChIP1. *Biochem. Biophys. Res. Commun.* 2003; **311**: 258–263.
15. Permyakov SE, Nazipova AA, Denesyuk AI, Bakunts AG, Zinchenko DV, Lipkin VN, Uversky VN, Permyakov EA. Recoverin as a redox-sensitive protein. *J. Proteome Res.* 2007; **6**: 1855–1863.
16. Hwang JY, Schlesinger R, Koch KW. Irregular dimerization of guanylate cyclase-activating protein 1 mutants causes loss of target activation. *Eur. J. Biochem.* 2004; **271**: 3785–3793.
17. Peshenki IV, Dizhoor AM. Activation and inhibition of photoreceptor guanylyl cyclase by guanylyl cyclase activation protein 1 (GCAP-1). The formation of Mg^{2+}/Ca^{2+} exchange in EF-hand domain. *J. Biol. Chem.* 2007; **282**: 21645–21652.
18. Chang LS, Lin SR, Chang CC, Yang CC. Disulfide isomerization within the C-terminus of cobrotoxin decelerates by thiol compounds and trintrophenylation, but accelerates by modification of carboxyl groups. *Arch. Biochem. Biophys.* 1998; **358**: 164–170.
19. Aravind P, Chandra K, Reddy PP, Jeromin A, Chary KVR, Sharma Y. Regulatory and structural EF-hand motifs of neuronal calcium sensor-1: Mg^{2+} modulates Ca^{2+} binding, Ca^{2+}-induced conformational changes, and equilibrium unfolding transitions. *J. Mol. Biol.* 2008; **376**: 1100–1115.

